Journal of Applied Science and Advanced Technology
Journal Homepage : https://jurnal.umj.ac.id/index.php/JASAT

Study of Fluid Flow Characteristics In A 90° Pipe Bend With Varying Guide Vane Length

James Julian[1*], Riki Hendra Purba[1], Khalees Sedeq[1], Fitri Wahyuni[1], Thomas Junaedi[2]
[1] *Department of Mechanical Engineering, Faculty of Engineering, Universitas Pembangunan Nasional Veteran Jakarta, Indonesia*
[2] *Faculty of Engineering, Universitas Muhammadiyah Jakarta, Indonesia*

ARTICLE INFO

JASAT use only:
Received date : 30 January 2024
Revised date : 21 February 2024
Accepted date : 26 May 2024

Keywords:
CFD,
Guide vane,
Pipe bend,
Reynolds number,
Velocity.

ABSTRACT

The influence of guide vane length and Reynolds number was investigated using computational fluid dynamics methods. By using a structured mesh, it is known that the three mesh variations used have been verified using the Richardson Extrapolation method. The validation process also showed quite good results. From this research, it can be seen from the velocity profile trend, which is close to the experimental results from previous studies. Changing the Reynolds number does not significantly change the velocity profile at the outlet bend. However, it can be seen that changes in the Reynolds number impact the fluid flow pattern produced around the pipe bend. It can be seen clearly, especially when the velocity is negative. Changing the length of the guide vane changes the flow pattern quite significantly. It is known that the shorter the guide vane used, the velocity profile will tend towards the outer core. Furthermore, using a guide vane increases the velocity profile at the position $-0.3 \leq r/R \leq -0.06$. Using a guide vane has proven to eliminate negative velocity areas on the inner core side of each variation.

Introduction

The piping system is complex and requires careful attention and consideration during the design process to produce the best and most effective piping system design [1]. This type of system is generally used in various industrial sectors, including the drinking water and oil industries. Piping systems include various components, such as straight pipes, flanges, valves, 90° pipe bends, and others. One essential component in a piping system is a 90° pipe bend [2]. 90° pipe bends are important in every pipe network because they provide flexibility and effectiveness in fluid distribution. The fluid distribution in a 90° bend pipe differs from that of a straight pipe. Various characteristics can be found in pipe bend 90, including fluid velocity fluctuations, fluid flow instability, flow separation, and secondary flow. The different Reynolds numbers, pipe diameters, and curvature ratios of the 90° pipe bend typically lead to diverse features of a 90° pipe bend.

* Corresponding author.
E-mail address: zames@upnvj.ac.id

Weske conducted experimental research regarding the velocity distribution in a 90° pipe bend using a variety of pipe cross-sectional shapes, such as circles, squares, and rectangles [3]. The analysis involved varying the Reynolds number value from 2×10^5 to 6×10^5. Sudo conducted experiments investigating turbulent flow in a 90° curved pipe with a curve ratio of Rc/D=2 [4]. A flat pipe segment, 100D in length, was positioned before the bend to induce turbulent flow in the curved pipe. The experiment used air as the medium with a Reynolds number of approximately 60,000. This study reveals phenomena occurring at different locations in the pipe, particularly at the curved section with an angle α=30°, where the secondary flow produces a pair of vortices. The method used involves using a hot-wire anemometer to measure flow velocity and velocity along the circumference of the pipe at several points along the pipe. Dutta investigated 90° pipe bends with high Reynolds numbers [5]. The approach used is computational simulation, which applies the k-epsilon turbulence model. The research results show that increasing the Reynolds number can return the velocity profile in the inner core region of the pipe to a fully formed flow, with a slowdown in the fluid flow velocity in

DOI: https://dx.doi.org/10.24853/JASAT.6.3.99-108

the outer region of the pipe core. The Reynolds number also impacts fluid flow separation in pipes, where an increase in the Reynolds number causes the flow separation to move upstream. On the other hand, with an increasing Reynolds number, the reattachment phenomenon moves downstream. A low-velocity area was detected in the core of the pipe bend, and this low-speed region became the starting point for flow separation. Julian studied pipe bend 90 with varying pipe bend curvature ratios, with a diameter (d) of 0.01 m [6]. As a result, at Rc/D=1 the fluid flow velocity moves from the inner core to the outer core, and flow separation is found. Meanwhile, at Rc/D=2 and Rc/D=3, no flow separation was found.

Overall, many studies related to 90°pipe ben have been carried out. In general, previous studies focused more on the effect of increasing the Reynolds number and the curvature ratio in a 90° pipe bend. The results of various previous studies showed that fluid flow in a 90° pipe bend will experience flow separation if Rc/D≤1.5 where Rc is the ratio of the pipe bend curvature and D is the pipe diameter. Flow separation is the cause of losses in flow in the pipe. So far, research focusing on using guide vanes is still scarce. Therefore, this research aims to compare the effect of guide vane length on the fluid flow characteristics in pipe bend 90. Furthermore, this research will also reveal the fluid flow characteristics in pipe bend 90, which have been given different guide vane length variations. Some characteristics studied include velocity profiles, fluid flow contours, and fluid flow streamlines.

Methods

Problem definition

The study focuses on analyzing the impact of varying the length of the guide vane along the pipe bend on fluid flow characteristics. The guide vane is positioned horizontally at the inlet of the bend in the hope of dividing the fluid flow radially. The geometry considered in this study focuses on pipe bend 90, with a diameter (D) of 0.01 m and a curvature ratio RC/D=1. The geometry is divided into four sections, each featuring a different guide vane configuration. The first section has a ¼ pipe bend guide vane, the second has a ½ pipe bend guide vane, the third has a ¾ pipe bend guide vane, and the fourth has a guide vane along the pipe bend. Each geometry has similar upstream and downstream sides; the upstream side measures 50D in length, while the downstream side measures 30D [5,7]. The geometry and shape of the guide vane are shown in Figure 1.

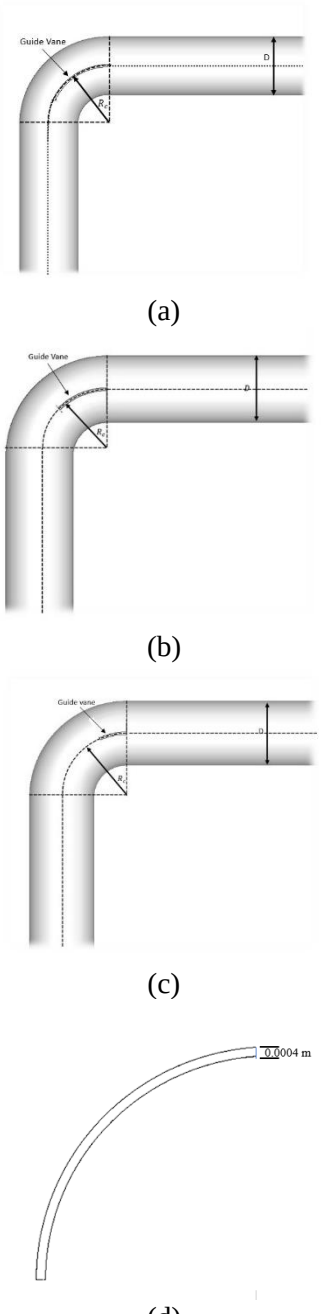

(a) (b) (c) (d)

Figure 1. (a) 90-degree pipe bend with ¾ guide vane, (b) 90-degree pipe bend with ½ guide vane, (c) 90-degree pipe bend with ¼ guide vane, (d) guide vane size

Meshing

The present study employs a three-dimensional structured mesh comprising hexahedral model elements. This mesh was chosen because it is suitable for simulation conditions that use 3D geometry, and its shape is simple enough. Meshing with this model makes computing time more effective, making iteration costs more economical

Journal of Applied Science and Advanced Technology 6 (3) pp 99-108 © 2024

[8,9]. Three types of mesh prepared for computing are divided based on the number of elements. The quantity of elements set is 5×10^5, 106, 2×10^6. The results of the mesh independence test determine terms of use for the number of meshes to be used. The mesh illustration for the current study is shown in Figure 2.

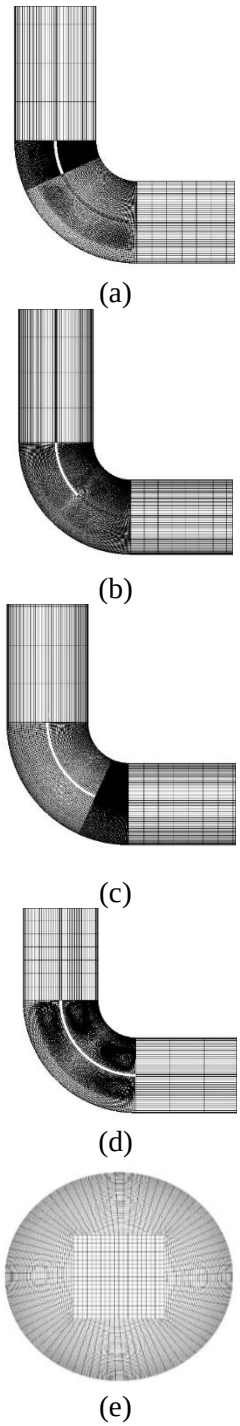

Figure 2. Meshing each pipe bend with varying lengths: (a) guide vane ¼, (b) guide vane ½, (c) guide vane ¾, (d) guide vane along pipe bend, (e) face meshing

Reynolds number

The Reynolds number, known as the Reynolds number, is a unitless numerical quantity used to evaluate the ratio between inertia and friction forces in a fluid. The mentioned value is used to analyze fluid flow characteristics, including laminar, transitional, or turbulent flow, by comparing the inertial and viscosity forces of the fluid [10]. The study at hand investigates different Reynolds numbers: 6×10^4, 7×10^4, and 8×10^4, and explores their variations.

$$R_e = \frac{\rho\, v\, d}{\mu} \tag{1}$$

Governing equations

The three-dimensional Reynolds Averaged Navier-Stokes (RANS) equations are solved via a separate implicit solving method. The selection of an appropriate turbulence model is significant in dealing with turbulent flows, especially in the context of three-dimensional flow phenomena that require accurate modeling. This study uses a second-order scheme to calculate the U-RANS equation, with pressure and velocity coupling obtained through a simple algorithm. The study utilized a time increment of 0.001 seconds, which spanned 1000 discrete time intervals. Uniform default relaxation factors were applied to ensure convergence for all models. In this research, the RANS equation is utilized to model incompressible flow. This is because the equation does not need to account for changes in density, as the density remains constant. The RANS equation for incompressible flows typically comprises two main equations: the mass conservation equation and the momentum conservation equation. The current study uses a working fluid in the form of water with a density of (ρ) 990.2 kg/m2 and a dynamic viscosity (μ) of 0.0006 kg/(m-s) [5,11].

$$\frac{\partial \rho}{\partial t} + \frac{\partial}{\partial x_i}(\rho u_i) = 0 \tag{2}$$

$$\frac{\partial}{\partial t}(\rho u_i) + \frac{\partial}{\partial x_i}(\rho u_i u_j) = -\frac{\partial \rho}{\partial x_i} + \frac{\partial}{\partial x_j}\left[\mu\left(\frac{\partial u_j}{\partial x_i} + \frac{\partial u_i}{\partial x_j} - \frac{2}{3}\delta_{ij}\frac{\partial u_j}{\partial x_j}\right)\right] + \frac{\partial}{\partial x_j}\left(\rho\overline{\dot{u}_i\, \dot{u}_j}\right) \tag{3}$$

Turbulence model

Because the fluid flow in a 90° pipe bend is investigated with the smallest Reynolds number 6×104, it can be concluded that the fluid flow in the

pipe is turbulent. Therefore, the current study uses a turbulence model to harmonize the RANS equations with turbulent flow. The choice of turbulence model can influence the results of the calculations. This study uses the standard k-ε turbulence model. This model can describe the turbulence characteristics of fluid flow in single-phase or two-phase flow quite well [12–17]. In this model, the dissipation rate of turbulence (ε) and turbulence kinetic energy (k) are resolved to determine the turbulent viscosity coefficient—transport equations for the k-epsilon turbulence model.

$$\frac{D}{D_t}(\rho k) = \frac{\partial}{\partial x_j}\left[\left(\mu + \frac{\mu_t}{\sigma_k}\right)\frac{\partial k}{\partial x_j}\right] + G_k - \rho\varepsilon \quad (4)$$

$$\frac{D}{D_t}(\rho \varepsilon) = \frac{\partial}{\partial x_j}\left[\left(\mu + \frac{\mu_t}{\sigma_\varepsilon}\right)\frac{\partial \varepsilon}{\partial x_j}\right] + C_{\varepsilon 1}\frac{\varepsilon}{k}G_k - \rho C_{\varepsilon 2}\frac{\varepsilon^2}{k} \quad (5)$$

Results and Discussions

The current study uses a mesh independence test. The method used in this test is Richardson extrapolation. Each step of mesh independence testing was carried out similarly to Julian's research [18–20]. The data characteristics for the mesh independence test use the velocity variable, taken at locations z=0.02, y=0, and x=0. Variations in the number of mesh elements are in the suitability index range where the independence test results $(GCI_{coarse})/(GCI_{fine}\ (r^p)\ ) \approx 1$. All test variables are presented in Table 1. The mesh-independent test results show that the smallest error percentage is the fine mesh with an error value of 0.0883%. Therefore, a mesh with several elements of 2×106 was used in this study. Figure 3 shows the results of the mesh-independent test.

Table 1. Mesh independence test

Mesh Categories	Number of Elements	Velocity	District Code	Error
Fine	2×10^6	5.999	f_1	0.0883%
Medium	1×10^6	5.975	f_2	0.4895%
Coarse	5×10^5	5.841	f_3	2.7135%

The data in this study must be validated first by comparing the results obtained with those of previous research or another research. The comparative data used is experimental research Kim and simulation research Dutta [5,13]. More detailed data validation results can be seen in Figure 4. Data was collected from a 90° pipe bend simulation with a curvature ratio R_c/D=2 during the validation process.

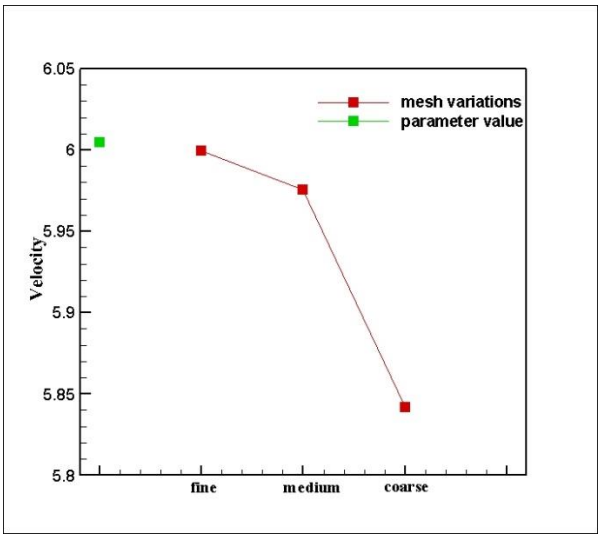

Figure 3. Mesh independence test result

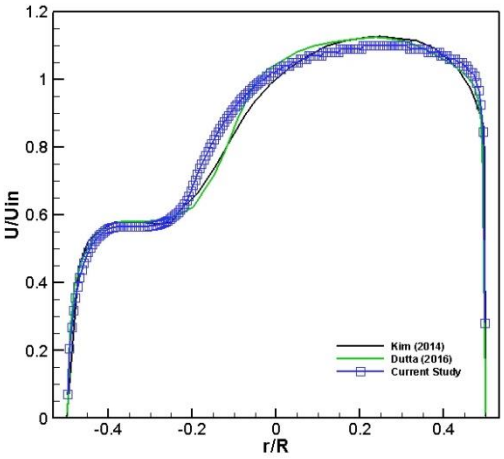

Figure 4. Validation results of the current study with other studies

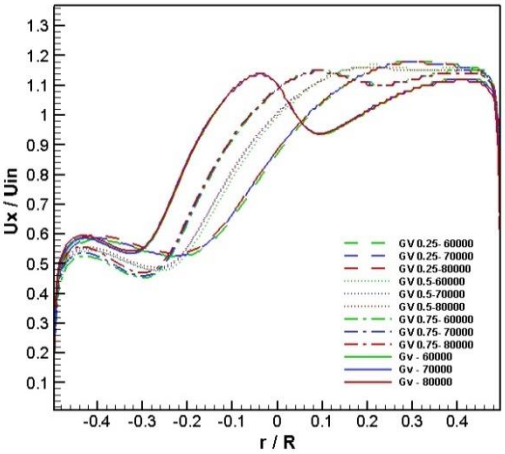

Figure 5. Velocity profile

Journal of Applied Science and Advanced Technology 6 (3) pp 99-108 © 2024

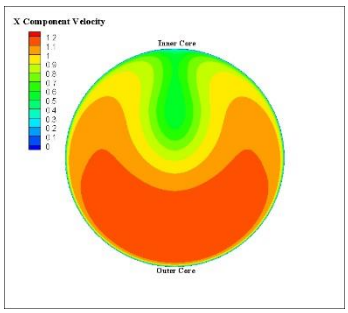

(a)

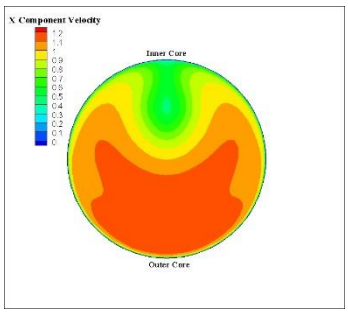

(b)

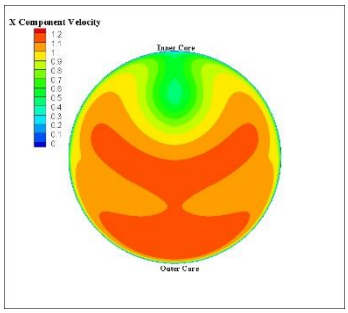

(c)

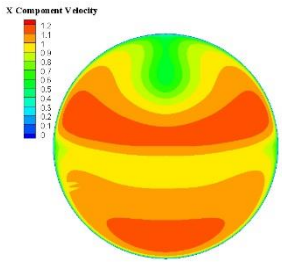

(d)

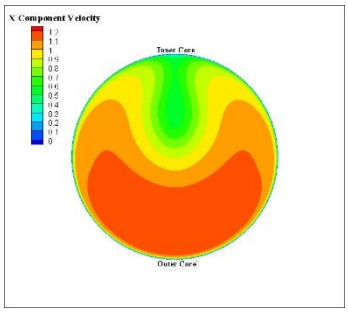

(e)

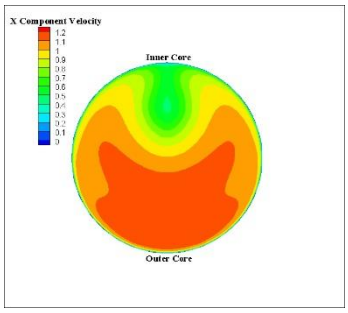

(f)

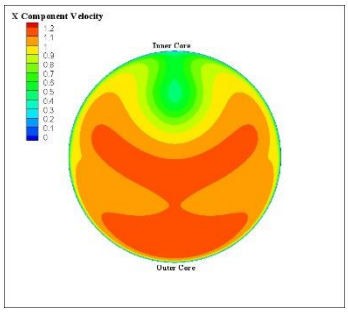

(g)

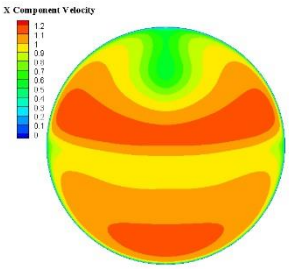

(h)

 e-ISSN : 2622 - 6553

(i) (j)

(k) (l)

Figure 6. Velocity contour at the inlet pipe bend with variations in guide bend length and Reynolds number (a) at Re =6×10^4 with guide vane ¼, (b) at Re =6×10^4 with guide vane½, (c) at Re =6×10^4 with guide vane¾, (d) at Re =6×10^4 with guide vane along pipe bend (e) at $Re = 7 \times 10^4$ with guide vane ¼, (f) at $Re = 7 \times 10^4$ with guide vane½, (g) at $Re = 7 \times 10^4$ with guide vane¾, (h) at $Re = 7 \times 10^4$ with guide vane along pipe bend, (i) at Re=8$\times 10^4$ with guide vane ¼, (j) at Re=8$\times 10^4$ with guide vane½, (k) at Re=8$\times 10^4$ with guide vane ¾, and (l) at Re=8$\times 10^4$ with guide vane along pipe bend

(a) (b)

(c) (d)

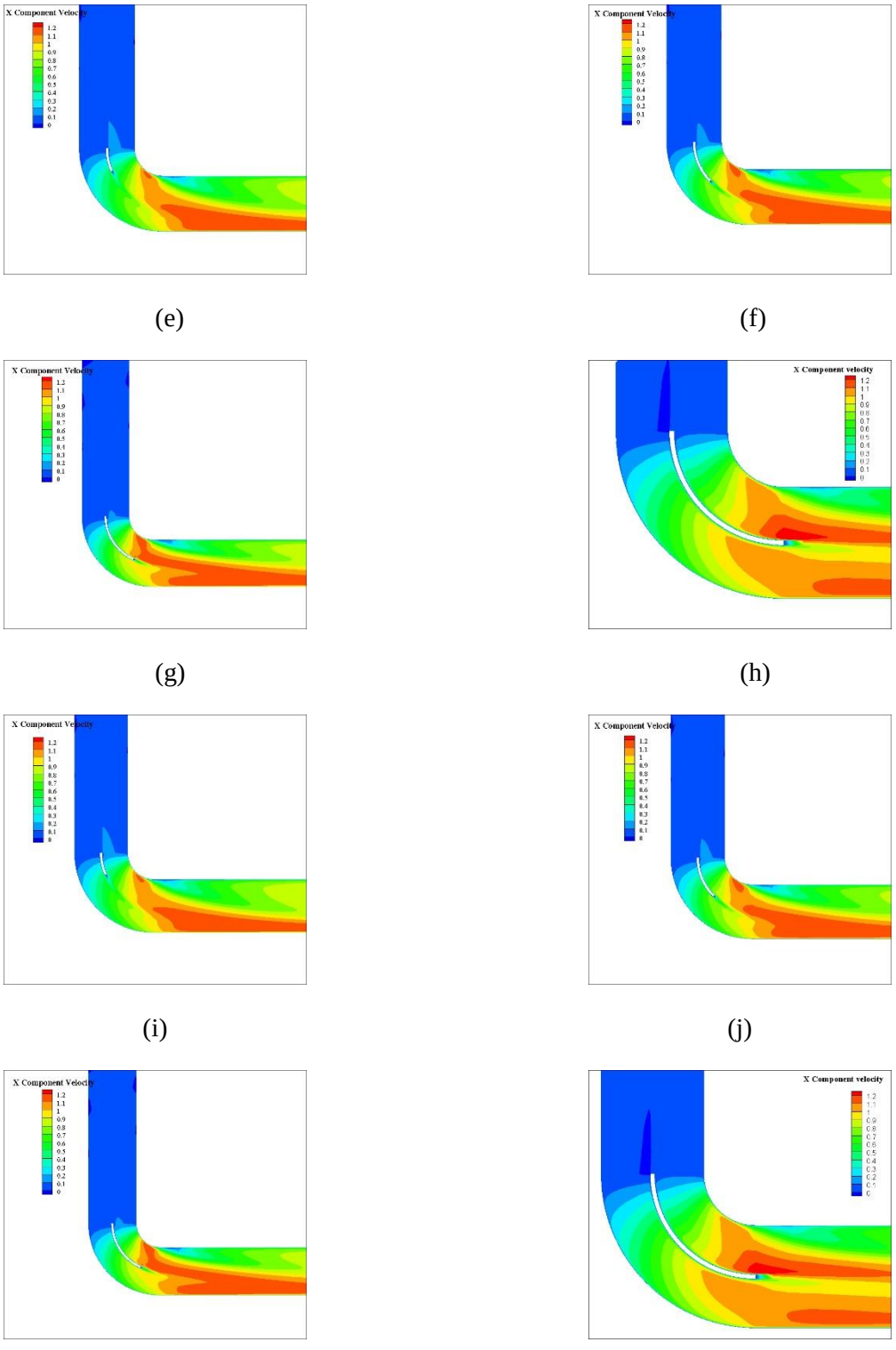

(e) (f)

(g) (h)

(i) (j)

(k) (l)

Figure 6. velocity contour along the pipe with variations in guide vane length and Reynolds number (a) at Re =6×10^4 with guide vane ¼, (b) at Re =6×10^4 with guide vane½, (c) at Re =6×10^4 with guide vane¾, (d) at Re =6×10^4 with guide vane along pipe bend (e) at $Re = 7 \times 10^4$ with guide vane ¼, (f) at $Re = 7 \times 10^4$ with guide vane½, (g) at $Re = 7 \times 10^4$ with guide vane¾, (h) at $Re = 7 \times 10^4$ with guide vane along pipe bend, (i) at Re=8×10^4 with guide vane ¼, (j) at Re=8×10^4 with guide vane½, (k) at

Re=8× 10^4 with guide vane ¾, and (l) at Re=8× 10^4 with guide vane along pipe bend

The main focus was on the velocity data obtained at the outlet of the pipe bend, specifically at a location of 0.02 sb z.Upon comparing the validation results with other studies, it becomes apparent that the existing data closely aligns with the two comparison datasets. This alignment is particularly noticeable within the ranges of r/R = -0.49 to r/R= -0.15 and r/R= 0 to r/R=0.49, demonstrating the data's strong suitability [5,13]. However, some validation data are not in identical positions, namely at r/R=-0.17 to r/R= 0. This data discrepancy may occur due to adverse pressure gradients in the inner core pipe bend area and differences in the use of fluent devices in computing. Thus, the data produced in this research can be said to be quite valid.

Each data display uses variations of the Reynolds number, with values of 6×10^4, 7×10^4, and 8×10^4. The analysis focused on the characteristics of the velocity profile, velocity fluctuations, and contours of the 90° baseline pipe bend with variations in the length of the guide vane.

The velocity profiles of four different geometries with varying guide vane lengths and Reynolds numbers are depicted in Figure 5. Across the three Reynolds numbers tested in each geometry, it is evident that the fluid velocity profile is not significantly affected by the Reynolds number. From the four geometries used, the length of the guide vane significantly influences the speed profile between the four geometries at $-0.5 \leq r/R \leq -0.2$. Meanwhile, at $-0.2 \leq r/R \leq 0.1$, guide vane length variations significantly affect the speed profile in that range. The study covers a range of 0.18 to 0.42 for r/R. Adjusting the length of the guide vane has a minor effect on the fluid flow velocity profile and causes a shift in the speed profile at r/R = -0.33. Additionally, guide vane lengths with geometries 3 and 4 result in decreased velocity profiles on the outer core side. These observations indicate that variations in the length of the guide vane can impact the fluid velocity profile at a 90° pipe bend.

The fluid inlet velocity normalizes the cross-sectional contour of the pipe bend outlet in Figure 6. The results indicate that as the guide vane length increases, the fluid flow distribution in the pipe becomes more precise and uniform. Specifically, using guide vane lengths of ¼ and ½ leads to uneven distribution between the inner and outer cores. Conversely, implementing a ¾ length guide vane and a guide vane along the pipe bend enhances flow distribution, as seen in the comparison. The flow equalization will become more evident as the Reynolds number increases. He continued using long guide vanes, which show that there are no low-speed areas on the inner and outer core.

Figure 7 presents the x-velocity contours of the four guide vane models. From each of the data displayed, the increase in the Reynolds number does not significantly affect each contour. At 90° pipe bends with different guide vane length variations, low-velocity areas remained on the inner core side. However, this area is not negative. He continued that as the Reynolds number increases, the low-speed region decreases and becomes smaller in each geometry. Of the four variations in guide vane length, it is obvious that the length of the guide vane significantly influences the contour of the 90° pipe bend.

Conclusion

The current research investigates the influence of varying guide vane lengths on velocity profile characteristics and fluid flow patterns at a 90° pipe bend. Employing the k-epsilon turbulence model with the RANS equation, the study examines three Reynolds numbers: 6×10^4, 7×10^4, and 8×10^4. The findings indicate that, contrary to expectations, the increase in Reynolds number does not significantly alter the velocity profile in each model. However, increasing the Reynolds number affects each contour produced. Increasing the Reynolds number reduces the low-speed region in each model. Variations in the length of the guide vane applied significantly affect the speed profile, where there is a shift in the speed profile towards the outer core side as the length of the guide vane used decreases. Variations in guide vane length also affect the flow distribution, which is divided between the outer and inner cores. Equalization will become more pronounced as the Reynolds number increases. Further varying the guide vane length increased the speed profile at $-0.3\leq r/R\leq -0.06$ in contrast, varying the length of the guide vane did not produce a negative velocity area on the inner core side in each geometry.

Acknowledgment

Thank you to all the authors who participated and contributed to the publication of this scientific work.

Journal of Applied Science and Advanced Technology 6 (3) pp 99-108 © 2024

Author Contributions

The authors' contributions to the paper are as follows: study conception, design, analysis, and interpretation of results: James Julian, Riki Hendra Purba; data collection: Fitri Wahyuni, Khalees Sedeq; draft manuscript preparation: Thomas Junaedi. All authors have reviewed the results and approved the final version of the manuscript.

Conflicts of Interest

All authors declare that they have no conflicts of interest.

References

[1] Husen A, Cholis N, Setiadi AN. Analisis tegangan pipa pada sistem instalasi perpipaan geothermal di proyek x. Bina Teknika 2018;14:63–77. https://doi.org/10.54378/bt.v14i1.297

[2] Malau J, Sitepu T. Analisa Pressure Drop pada Sistem Perpipaan Fuel Oil Boiler pada PT. PLN Pembangkitan Sumatera Bagian Utara Sicanang–Belawan dengan Menggunakan Pipe Flow Expert. Jurnal E-Dinamis 2012;3:164–71. http://dx.doi.org/10.12962/j23373539.v7i1.28397

[3] Weske JR. Experimental investigation of velocity distributions downstream of single duct bends. National Advisory Committee for Aeronautics; 1948. http://dx.doi.org/10.2298/TSCI230816244M

[4] Sudo K, Sumida M, Hibara Hje. Experimental investigation on turbulent flow in a circular-sectioned 90-degree bend. Exp Fluids 1998;25:42–9. https://doi.org/10.1007/s003480050206

[5] Dutta P, Saha SK, Nandi N, Pal N. Numerical study on flow separation in 90° pipe bend under high Reynolds number by k-ε modelling. Engineering Science and Technology, an International Journal 2016;19:904–10. https://doi.org/10.1016/j.jestch.2015.12.005

[6] Julian J, Wahyuni F, Iskandar W, Ramadhani R. The effect of curvature ratio towards the fluid flow characteristics in bend pipe based on numerical methods. Turbo: Jurnal Program Studi Teknik Mesin 2023;12. http://dx.doi.org/10.24127/trb.v12i1.2564

[7] Reghunathan Valsala R, Son SW, Suryan A, Kim HD. Study on reduction in pressure losses in pipe bends using guide vanes. J Vis (Tokyo) 2019;22:795–807. https://doi.org/10.1007/s12650-019-00561-w

[8] Du Y, Ekaterinaris JA. Time-marching schemes for spatially high order accurate discretizations of the Euler and Navier–Stokes equations. Progress in Aerospace Sciences 2022;130:100795. https://doi.org/10.1016/j.paerosci.2021.100795

[9] Iskandar W, Julian J, Wahyuni F, Ferdyanto F, Prabu H, Yulia F. Study of Airfoil Characteristics on NACA 4415 with Reynolds Number Variations. International Review on Modelling and Simulations (IREMOS) 2022;15:162. https://doi.org/10.15866/iremos.v15i3.21684.

[10] Erlangga GP. Studi Eksperimental Karakteristik Aerodinamik Airfoil Naca 4412 Dengan Variasi Kecepatan Aliran Udara. Departemen Teknik Fisika, Fakultas Teknologi, Industri Institut Teknologi Sepuluh Nopember, Surabaya 2017. https://doi.org/10.14710/rotasi.21.3.147-154

[11] Julian J, Iskandar W, Wahyuni F. Effect of Single Slat and Double Slat on Aerodynamic Performance of NACA 4415. vol. 7. 2022. https://doi.org/10.12962/j25481479.v7i2.12875

[12] Homicz GF. Computational Fluid Dynamic simulations of pipe elbow flow. Sandia National Laboratories (SNL), Albuquerque, NM, and Livermore, CA …; 2004. https://doi.org/10.2172/919140

[13] Kim J, Yadav M, Kim S. Characteristics of secondary flow induced by 90-degree elbow in turbulent pipe flow. Engineering Applications of Computational Fluid Mechanics 2014;8:229–39. https://doi.org/10.1080/19942060.2014.11015509

[14] Julian J, Iskandar W, Wahyuni F, Bunga NT. Aerodynamic Performance Improvement on NACA 4415 Airfoil by Using Cavity. Jurnal Asiimetrik: Jurnal Ilmiah Rekayasa Dan

Inovasi 2023;5. https://doi.org/10.35814/asiimetrik.v5i1.4259

[15] Leonov K, Akhatov I. The influence of dissolved gas on dynamics of a cavitation bubble in an elastic micro-confinement. Int J Heat Mass Transf 2022;196:123295. https://doi.org/https://doi.org/10.1016/j.ijheatmasstransfer.2022.123295

[16] Julian J, Iskandar W, Wahyuni F. Leading Edge Modification of NACA 0015 and NACA 4415 Inspired by Beluga Whale. International Journal of Marine Engineering Innovation and Research 2023;8. https://doi.org/10.12962/j25481479.v8i2.16432

[17] Julian J, Iskandar W, Wahyuni F. Aerodynamics Improvement of NACA 0015 by Using Co-Flow Jet. International Journal of Marine Engineering Innovation and Research 2022;7:1479–2548. https://doi.org/10.12962/j25481479.v7i4.14898

[18] Julian J, Iskandar W, Wahyuni F, Armansyah A, Ferdyanto F. Effect of single slat and double slat on aerodynamic performance of NACA 4415. International Journal of Marine Engineering Innovation and Research 2022;7. https://doi.org/10.12962/j25481479.v7i2.12875

[19] Julian J, Anggara RA, Wahyuni F, Bunga NT. The The Effect of Micro Geometry with Various Forms as Passive Flow Control in NACA 4415. Jurnal Asiimetrik: Jurnal Ilmiah Rekayasa Dan Inovasi 2023;5. https://doi.org/10.35814/asiimetrik.v5i2.4678

[20] Julian J, Siswanto SA, Wahyuni F, Bunga NT. Analysis of the Use of Bio Flap on NACA 4415 with Numerical Methods. Jurnal Asiimetrik: Jurnal Ilmiah Rekayasa Dan Inovasi 2023;5. https://doi.org/10.35814/asiimetrik.v5i2.4768